

## Hybrid simulation of toroidal Alfvén eigenmode on the National Spherical Torus Experiment

D. Liu, G. Y. Fu, N. A. Crocker, M. Podestà, J. A. Breslau, E. D. Fredrickson, and S. Kubota

Citation: *Physics of Plasmas* **22**, 042509 (2015); doi: 10.1063/1.4917523

View online: <http://dx.doi.org/10.1063/1.4917523>

View Table of Contents: <http://scitation.aip.org/content/aip/journal/pop/22/4?ver=pdfcov>

Published by the [AIP Publishing](#)

---

### Articles you may be interested in

[Properties of Alfvén eigenmodes in the Toroidal Alfvén Eigenmode range on the National Spherical Torus Experiment-Upgrade](#)

*Phys. Plasmas* **20**, 082502 (2013); 10.1063/1.4817277

[Nonlinear simulation of toroidal Alfvén eigenmode with source and sink](#)

*Phys. Plasmas* **17**, 042309 (2010); 10.1063/1.3394702

[Modeling fast-ion transport during toroidal Alfvén eigenmode avalanches in National Spherical Torus Experiment](#)

*Phys. Plasmas* **16**, 122505 (2009); 10.1063/1.3265965

[Alfvén cascade modes at high  \$\beta\$  in the National Spherical Torus Experiment](#)

*Phys. Plasmas* **15**, 102502 (2008); 10.1063/1.2993182

[Beam ion driven instabilities in the National Spherical Tokamak Experiment](#)

*Phys. Plasmas* **11**, 2586 (2004); 10.1063/1.1689667

---



**PFEIFFER VACUUM**

**VACUUM SOLUTIONS FROM A SINGLE SOURCE**

Pfeiffer Vacuum stands for innovative and custom vacuum solutions worldwide, technological perfection, competent advice and reliable service.

**125 YEARS NOTHING IS BETTER**

# Hybrid simulation of toroidal Alfvén eigenmode on the National Spherical Torus Experiment

D. Liu,<sup>1,a)</sup> G. Y. Fu,<sup>2</sup> N. A. Crocker,<sup>3</sup> M. Podestà,<sup>2</sup> J. A. Breslau,<sup>2</sup> E. D. Fredrickson,<sup>2</sup> and S. Kubota<sup>3</sup>

<sup>1</sup>*Department of Physics and Astronomy, University of California, Irvine, California 92697, USA*

<sup>2</sup>*Princeton Plasma Physics Laboratory, Princeton, New Jersey 08543, USA*

<sup>3</sup>*Department of Physics and Astronomy, University of California, Los Angeles, California 90095, USA*

(Received 16 January 2015; accepted 2 April 2015; published online 14 April 2015)

Energetic particle modes and Alfvén eigenmodes driven by super-Alfvénic fast ions are routinely observed in neutral beam heated plasmas on the National Spherical Torus eXperiment (NSTX). These modes can significantly impact fast ion transport and thus cause fast ion redistribution or loss. Self-consistent linear simulations of Toroidal Alfvén Eigenmodes (TAEs) in NSTX plasmas have been carried out with the kinetic/magnetohydrodynamic hybrid code M3D-K using experimental plasma parameters and profiles including plasma toroidal rotation. The simulations show that unstable TAEs with  $n = 3, 4$ , or  $5$  can be excited by the fast ions from neutral beam injection. The simulated mode frequency, mode radial structure, and phase shift are consistent with measurements from a multi-channel microwave reflectometer diagnostic. A sensitivity study on plasma toroidal rotation, safety factor  $q$  profile, and initial fast ion distribution is performed. The simulations show that rotation can have a significant destabilizing effect when the rotation is comparable or larger than the experimental level. The mode growth rate is sensitive to  $q$  profile and fast ion distribution. Although mode structure and peak position depend somewhat on  $q$  profile and plasma rotation, the variation of synthetic reflectometer response is within experimental uncertainty and it is not sensitive enough to see the difference clearly. © 2015 AIP Publishing LLC.

[<http://dx.doi.org/10.1063/1.4917523>]

## I. INTRODUCTION

In ITER and future fusion devices, fast or energetic ions generated by fusion reactions or auxiliary heating systems need to be sufficiently well confined so that their energy can be transferred to thermal plasmas to maintain fusion burn.<sup>1,2</sup> One great challenge concerns fast ion driven instabilities and toroidal magnetic field ripples since they could cause significant fast ion losses, lead to serious damage to plasma facing components, and degrade plasma performance.<sup>3</sup> Among fast ion driven instabilities, Alfvén type instabilities such as Toroidal Alfvén Eigenmodes (TAEs)<sup>4–6</sup> are of primary concern and interest since they can significantly enhance fast ion radial transport.<sup>7</sup> It is crucial to understand and possibly control the behavior of the fast ion population and associated instabilities.<sup>2</sup> The tools of modeling energetic particle physics have reached a stage at which it is possible to make quantitative comparisons with experiments. Many first-principle numerical simulation codes are being benchmarked or validated with experiments<sup>8–11</sup> in order to improve the predictive capability of fast ion driven instabilities and transport in burning plasmas. In this paper, a validation of the global kinetic/magnetohydrodynamic (MHD) hybrid code M3D-K<sup>12</sup> is carried out for the unstable TAEs observed in a weakly reversed magnetic shear and neutral-beam-heated discharge in the National Spherical Torus eXperiment (NSTX).<sup>13</sup>

The TAE modes exist with discrete frequencies located inside the shear Alfvén continuum gaps induced by toroidal

coupling of adjacent poloidal harmonics. The main drive is the radial gradient of the fast ion distribution. Because of the broad radial structure, relatively low instability threshold, and resonant interaction with fast ions, TAE modes can potentially cause substantial fast-ion redistribution or loss. NSTX, a medium size and low aspect ratio spherical torus, is an excellent test-bed to study fast ion driven instabilities. Because of the relatively weak toroidal magnetic field ( $B_t < 0.55$  T), fast ions generated by three co-current Neutral Beam Injections (NBI), with tangency radii of 0.69, 0.59, 0.49 m and energies from 65 to 90 keV, are super-Alfvénic, and they can easily drive a wide variety of MHD and Alfvén eigenmode instabilities, ranging from low-frequency ( $< 50$  kHz) fishbone and other kink-like modes, 70 – 120 kHz TAEs, up to  $\approx 2.5$  MHz Compressional Alfvén Eigenmodes (CAEs) and Global Alfvén Eigenmodes (GAEs).<sup>14</sup> Although the typical scenarios on NSTX are considerably different from those predicted for ITER and future fusion reactors, the dimensionless physics parameters for fast ion physics, in terms of the fast-ion beta normalized to the total beta and the fast-ion velocity normalized to the Alfvén speed, significantly overlap with the parameters of conventional aspect ratio tokamaks and future fusion reactors.<sup>15</sup> The discharges on NSTX provide good test cases to challenge present theories and numerical codes across a large range of different plasma conditions. Comparisons between experimental measurements and linear MHD calculation of TAE properties on NSTX have been previously explored with the linear ideal MHD eigenvalue code NOVA.<sup>16–18</sup> Although the modeled mode structure qualitatively agrees with the

<sup>a)</sup>Electronic mail: deyongl@uci.edu

measurements, these modelings did not include non-perturbative kinetic effects of fast ions. In this work, the global kinetic/MHD hybrid code M3D-K is employed, in which the thermal plasma is described by resistive MHD while the energetic ion species is treated by the drift-kinetic equation. The model is self-consistent including the kinetic effects of wave particle resonances. It computes the initial value solutions of the kinetic/MHD equations in toroidal geometry. The M3D-K code has been used successfully in simulating TAEs in a tokamak equilibrium with circular flux surfaces,<sup>19</sup> tearing modes in a low beta tokamak plasma,<sup>20</sup> kink modes and fishbones in ITER and NSTX,<sup>12,21,22</sup> and fast-ion-driven Reversed Shear Alfvén Eigenmodes (RSAE) in the DIII-D Tokamak.<sup>23</sup> In the present work, we mainly focus on the linear simulations of fast ion driven TAEs on NSTX for the purpose of code validation. Nonlinear simulations of TAEs with M3D-K are currently underway and will be reported in the future.

This paper is organized as follows. In Sec. II, simulation model and input plasma parameters and profiles are described. In Sec. III, the linear simulation results of  $n = 3, 4,$  and  $5$  TAEs are presented. The simulated mode frequency and mode structure are compared with experimental measurements. In Sec. IV, a sensitivity study of mode radial structure and mode frequency on plasma toroidal rotation, safety factor  $q$  profile, and initial fast ion distribution is performed and their effects are discussed. Section V summarizes the main results and discusses the future work.

## II. SIMULATION SETUP

The plasma parameters and equilibrium profiles used in the simulation are taken from experimental data of the NSTX NBI-heated discharge #141711, the same discharge that has been extensively analyzed with NOVA-K code in Ref. 17. This is an L mode deuterium discharge with excellent diagnostic coverage. As shown in the spectrogram of magnetic fluctuation (Fig. 1), bursting TAEs with duration of  $\sim 1$  ms started to appear around  $t = 405$  ms during the 90 kV, 2 MW neutral beam injection, evolved into large bursts with frequency down-chirp, and eventually led to a TAE avalanche between  $t = 480$  and  $485$  ms. During the TAE avalanche, a significant population of fast ions was lost or redistributed, as indicated by neutron rate drop. In addition, it was observed that the  $n = 2, 3, 4, 5$  TAE mode structure did not change significantly during the TAE bursting periods and even during the avalanche.<sup>17</sup>

The time slice of  $t = 470$  ms, about 10 ms before the TAE avalanche, is chosen for the M3D-K linear simulation of TAEs on NSTX. The observed changes in the mode amplitude and frequency around the slice of interest were relatively small compared with the changes during TAE avalanche. The main input parameters for the M3D-K calculations are major radius  $R = 0.85$  m, minor radius  $a = 0.67$  m, toroidal central magnetic field  $B_0 = 0.53$  T, central plasma density  $n_0 = 4.7 \times 10^{13} \text{ cm}^{-3}$ , central electron temperature  $T_e(0) = 1.4$  keV and ion temperature  $T_i(0) = 1.3$  keV, and Alfvén speed  $v_A \equiv \frac{B_0}{(n_0 m_i \mu_0)^{1/2}} = 1.19 \times 10^6$  m/s. In the M3D-K

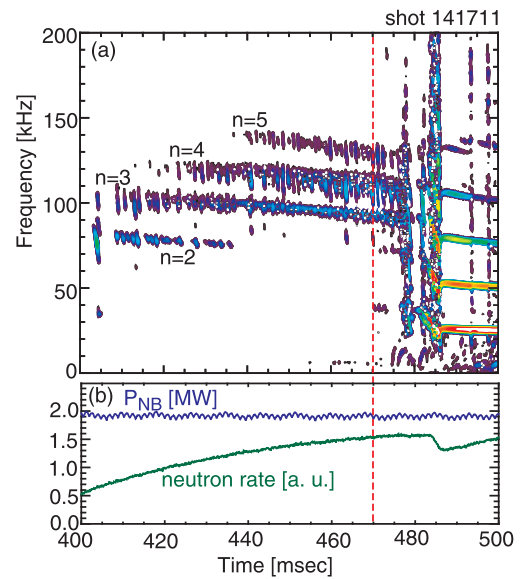


FIG. 1. (a) Spectrogram of magnetic fluctuations from Mirnov coils showing  $n = 2, 3, 4,$  and  $5$  TAEs for the discharge 141711. (b) Waveforms of neutral beam power and neutron rate. The time slice at  $t = 470$  ms, marked with dashed red line, is chosen for M3D-K simulations.

simulations, the on-axis thermal plasma beta is  $\beta_{thermal} = 0.195$  and fast ion beta is  $\beta_f = 0.117$ . Figure 2 shows the normalized thermal plasma pressure, fast ion pressure, plasma density,  $q$  profile, and toroidal rotation profile as a

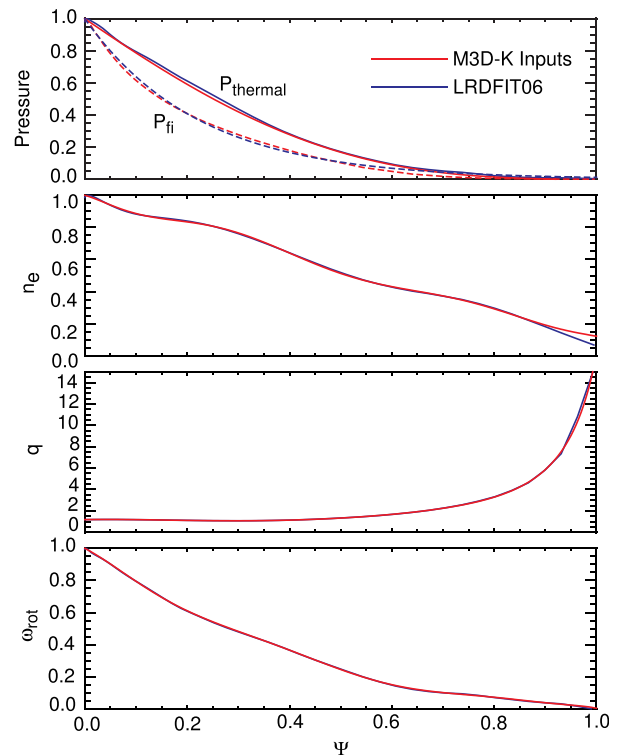


FIG. 2. Equilibrium profiles of (a) thermal pressure and fast ion pressure, (b) plasma density, (c) safety factor  $q$ , (d) toroidal rotation are plotted as functions of normalized poloidal flux  $\psi$ . The thermal pressure, fast ion pressure, plasma density, and the rotation profiles are normalized to unity at the magnetic axis. Note the red lines are the M3D-K inputs and blue lines that overlapped with red lines are experimental data from equilibrium reconstruction LRDFIT06 or TRANSP run with LRDFIT06 equilibrium.

function of normalized poloidal flux  $\psi$ . The fast ion pressure profile is calculated by the NUBEAM<sup>24</sup> module in the transport analysis code TRANSP<sup>25</sup> assuming fast ions behave classically. The equilibrium geometry, magnetic field, pressure, and density profiles are all obtained through the Grad-Shafranov equilibrium reconstruction code LRDFIT,<sup>26</sup> which is constrained by magnetic data and the Motional Stark effect (MSE)<sup>27</sup> measurements of magnetic pitch. As shown in Fig. 2(c), the magnetic shear is weakly reversed with minimum of  $q$ ,  $q_{min} = 1.07$ , located at  $\psi = 0.30$ . The uncertainty in the  $q$  reconstruction is  $\Delta q \simeq 0.1$ , mostly caused by different choices of the constraints imposed in the solution of the Grad-Shafranov equilibrium. The initial fast ion distribution in the M3D-K simulations is a slowing-down distribution in energy and a peaked distribution in pitch angle,<sup>12</sup> i.e.,  $f = \frac{cH(v_0-v)}{v^3+v_c^3} \exp(-\langle\psi\rangle/\Delta\psi) \exp(-\frac{(\Lambda-\Lambda_0)^2}{\Delta\Lambda^2})$ , where  $c$  is a normalization factor,  $H$  is the Heaviside function,  $v_0$  is the maximum fast ion speed,  $v_c$  is critical speed at which equal amounts of energy are transferred from the fast ions to the background ions and electrons,  $\langle\psi\rangle$  is  $\psi$  averaged over the particle orbit, and  $\Lambda \equiv \mu B_0/E$ . The fast ion maximum speed is  $v_0/v_A = 2.49$ , corresponding to the neutral beam injection energy 90 keV. The critical speed of fast ion is  $v_c/v_A = 0.60$ , estimated with central plasma density and temperature. The maximum fast ion gyroradius is  $\rho_f/a = 0.174$ . The electrostatic potential related with plasma toroidal rotation is not considered in the loading of initial fast ion distribution.

The baseline case for the  $n=3$  TAE simulations in the rest of this paper is one for which  $q_{min} = 1.07$  at  $\psi = 0.30$ , central toroidal rotation  $\Omega_0 = 0.245$ , which are best fit to experimental measurements. For the initial fast ion distribution, central pitch  $\Lambda_0 = 0.60$  and pitch width  $\Delta\Lambda = 0.30$ , which is a good approximation to the full energy component of fast ion distribution in co-current neutral beam injection scenarios in NSTX. It should be pointed out that although the spatial profile of TRANSP calculated fast ion distribution is used, the input initial fast ion distribution could still be different from real fast ion distribution in phase space because the fast ions from deuterium neutral beams in experiments always have three energy components, while only the full energy component is considered in the M3D-K calculations. In addition, the modification of fast ion distribution due to TAEs is not included in TRANSP calculation. The numbers of radial mesh grids for  $n=3, 4$ , and  $5$  TAE simulations are 101, 121, and 121, and simulation particle numbers are  $2 \times 10^7$ ,  $2 \times 10^7$ , and  $4 \times 10^7$ , respectively. The time step is  $\Delta t = 0.00625t_A$  with  $t_A = R/v_A$  being the Alfvén time. A systematic convergence study has been performed by varying the spatial resolution as well as time step size and number of particles. It is found that this numerical resolution and particle numbers are adequate for the results to be shown below.

### III. LINEAR SIMULATION OF TOROIDAL ALFVÉN EIGENMODE

As the first step to validate the M3D-K code, we carried out three linear simulations with toroidal mode  $n=3, 4$ , and  $5$ , respectively. Fig. 3 shows the eigenmode

structure of stream function  $U$  and perturbed parallel fast ion pressure  $\delta P_{\parallel}$  in the poloidal cross section, where  $U$  is the stream function of the incompressible part of the perturbed plasma velocity. It is observed that the modes are mainly localized in the low field side of the magnetic axis, i.e., ballooning feature, with a twisted character. The dominant harmonics are  $(n=3, m=3)$ ,  $(n=4, m=4)$ ,  $(n=5, m=5)$  for  $n=3, 4$ , and  $5$  cases, respectively. In addition, the calculated mode frequency is compared with the measured frequency that is obtained from the spectrogram of Mirnov coil signals. As shown in Fig. 4, the simulated frequency is close to the measured frequency within discrepancy less than 10 kHz. Note that both the simulated and measured frequencies are in the lab frame, i.e., Doppler shift has been included. The  $n=3, 4$ , and  $5$  modes observed in Fig. 1 at  $t = 470$  ms were identified as TAEs based on their frequencies and toroidal mode numbers.<sup>17</sup> The measured mode frequencies are reasonably close to the nominal TAE gap frequencies when taking into account the measured modes numbers and toroidal Doppler shift. Both the good agreement between M3D-K calculated and measured TAE mode frequencies and the ballooning feature exhibited in Fig. 3 suggest that these unstable modes found by M3D-K simulations are TAEs. In the  $n=1$  case, the calculated mode structure and mode frequency indicate that it is a kink-like mode, not a TAE mode. This is consistent with experimental observations that there are mainly  $n=3, 4$ , and  $5$  TAEs at  $t = 470$  ms.

Furthermore, the simulated mode structure is compared with the measurements from a multi-channel reflectometry diagnostic.<sup>28</sup> The reflectometry measures the path length variation of a probe microwave signal resulting from plasma density fluctuations. Based on the path length variation, an estimate of cutoff density contour displacement can be obtained, which is approximately the radial plasma displacement when there is no compression (see Ref. 28, and references therein). With density fluctuation obtained from M3D-K simulations and equilibrium plasma density, a simple one-dimensional synthetic reflectometry diagnostic is used to simulate the reflectometry path length fluctuation caused by the mode. The synthetic diagnostic assumes small density fluctuation around the unperturbed equilibrium density profile and uses the O-mode path length integral to calculate the perturbation caused by the mode. Figure 5 compares the effective reflectometry radial displacement,<sup>28</sup>  $|d\xi|$  defined as half the path length fluctuation, from measurements and M3D-K simulations. Although the simulated mode peak positions slightly shift inward a few cm compared with measurements, the simulated mode structure is reasonably consistent with measurements considering  $\sim 10\%$  uncertainties in the input  $q$  and density profiles and relatively large uncertainties in the fast ion density distribution function. Note that the simulation results here are from linear M3D-K simulations. The perturbed density is less than  $\sim 0.1\%$  of equilibrium plasma density, and thus the reflectometer response scales linearly with the perturbed density. For convenience of comparison, the magnitude of simulated reflectometer response is re-scaled until the peak magnitude

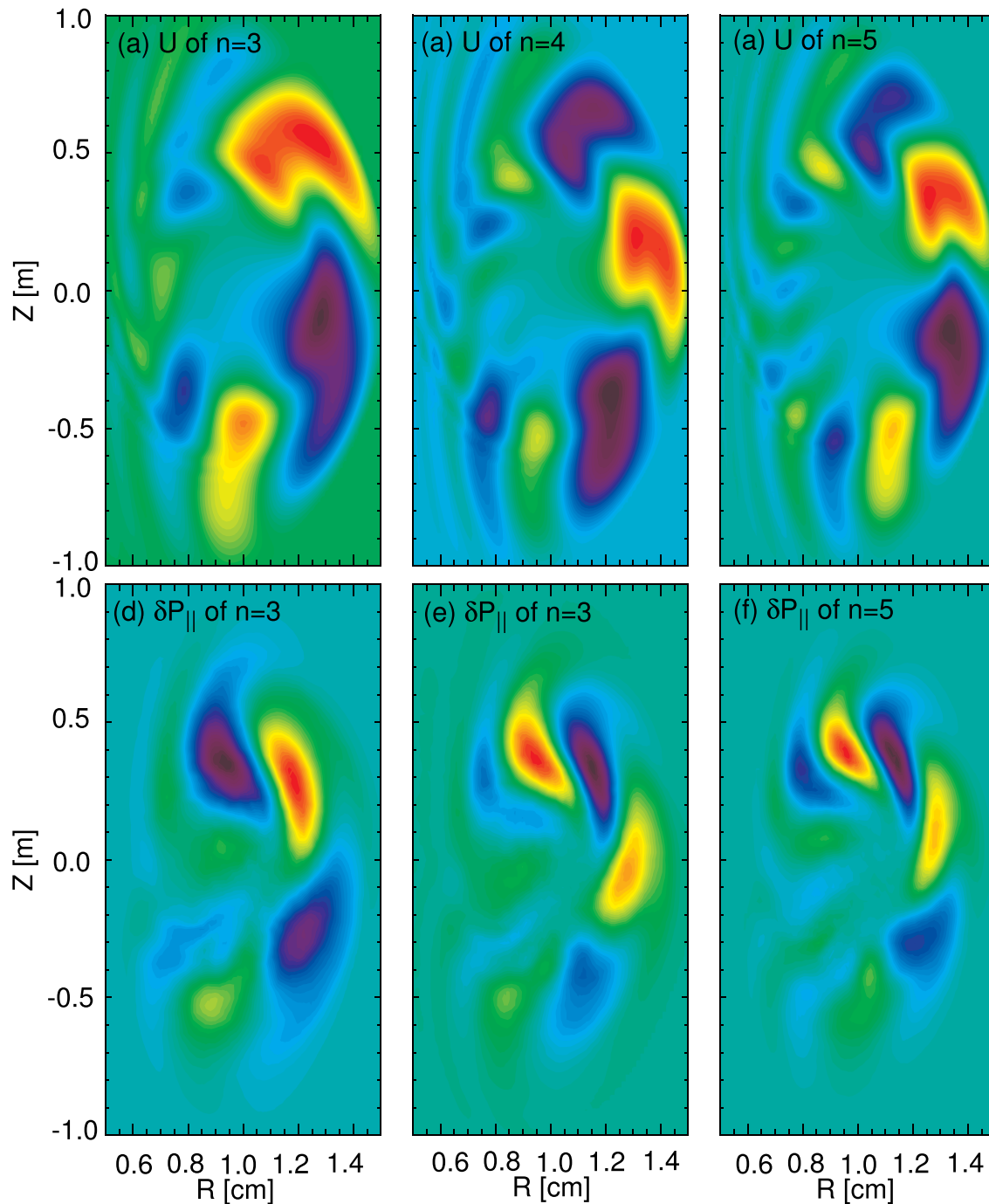


FIG. 3. Contour plots of velocity streaming function  $U$  and pressure perturbation  $\delta P_{\parallel}$  from  $n = 3, 4,$  and  $5$  linear M3D-K simulations.

matches with the peak of measurements for all linear M3D-K simulations presented in this work.

#### IV. SENSITIVITY STUDY OF TAE MODE STRUCTURE AND MODE FREQUENCY DUE TO EXPERIMENTAL UNCERTAINTIES

In Section III, we have presented the M3D-K simulation results of fast ion driven TAEs with typical NSTX experimental parameters. Here we examine whether and how experimental uncertainties affect the simulation results. The most important ones are the uncertainties in the fast ion

distribution,  $q$  profile, and toroidal rotation. The radial gradient of fast ion distribution determines the amount of free energy available to drive TAEs. The fast ion density distribution is not well determined experimentally since the signals of fast ion diagnostics are typically integrated over certain portions of real space or phase space. In the M3D-K simulations, the TRANSP calculated fast ion pressure profile is used. Although the TRANSP calculated fast ion distribution is quite accurate in quiescent plasmas,<sup>29</sup> it could be significantly different from the real distribution during MHD or Alfvén instabilities since anomalous fast ion transport is not included in our TRANSP runs. It should also be pointed out

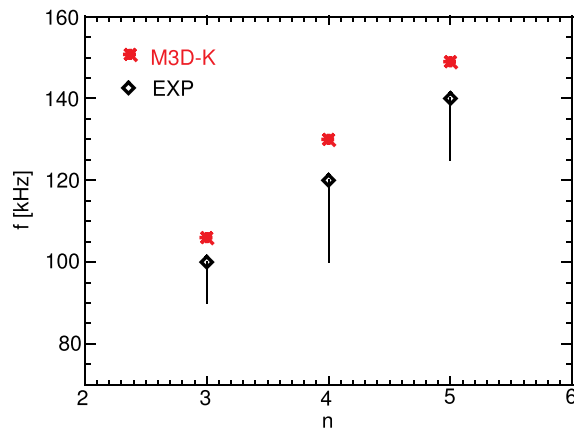


FIG. 4. Comparison of simulated and measured TAE frequencies. Red asterisk points represent the TAE frequencies at the mode peak position from M3D-K simulations, while black diamond points with vertical lines are the TAE frequencies obtained from the spectrogram of Mirnov coils. The solid vertical lines show the measured frequency range when the frequency chirps down during TAE bursts.

that in M3D-K simulations, only the spatial profile in real space fits to the TRANSP output, but the velocity distribution in phase space uses an analytical slowing-down form for the full energy component only. Therefore the input fast ion distribution and radial gradient are poorly constrained by experimental measurements, and the uncertainties are quite large. The  $q$  profile and rotation profile determine the Alfvén continuum gap structures and hence the mode structure. The  $q$  profile has an uncertainty of  $\sim 10\%$  and the  $q_{min}$  position and values are not very accurate. The toroidal rotation can modify the structure of the Alfvén continuum via the Doppler shift, and in some cases, the rotation shear can cause

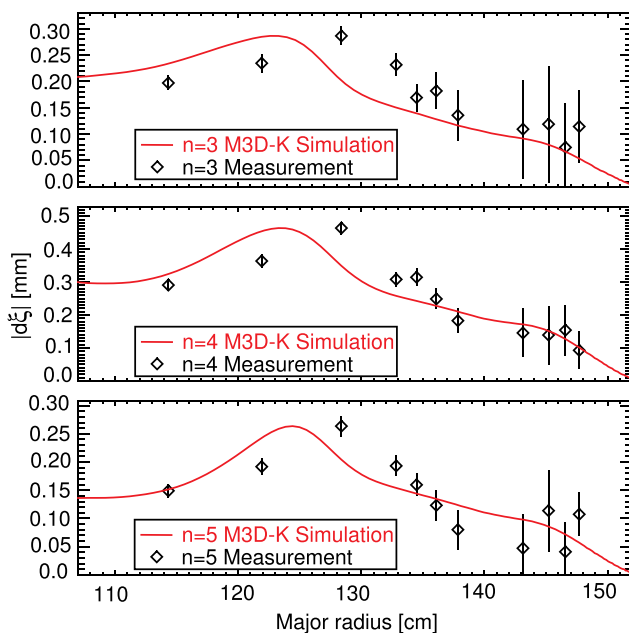


FIG. 5. Comparison between measured (diamonds with error bars, black) and M3D-K simulated (red line) reflectometer effective radial displacement for  $n=3, 4,$  and  $5$  TAEs. Experimental plasma profiles at  $t = 470$  ms are used for the M3D-K simulation, and reflectometry data are averaged in the window of  $469\text{--}470$  ms.

deformation of the radial structure of the TAE mode. The experimental rotation profile is inferred from the Doppler shift of the C VI line with a charge-exchange recombination spectroscopy system.<sup>30</sup> The uncertainty is  $1\text{--}2$  km/s in the core although it is quite large near the edge.

A sensitivity study is performed for the  $n=3$  TAE simulation case to check the effects of fast ion distribution,  $q$  profile, and toroidal rotation on the mode peak position and mode structure. Varying the fast ion central pressure  $\beta_{fi}(0)$ , we observe a near-linear scaling in Fig. 6 between the normalized mode growth rate  $\gamma/\omega_{alfven}$  and  $\beta_{fi}(0)$ , where  $\omega_{alfven} = v_A/R$  is Alfvén frequency. The near-linear scaling is easy to understand since fast ions are the driving source. When extrapolated back to zero growth rate, it is found the  $n=3$  TAE starts to become unstable when  $\beta_{fi}(0)/\beta_{thermal}(0) > 0.45$ , i.e.,  $\beta_{fi}(0)/\beta_{total}(0) > 0.31$ . This is reasonably consistent with the experimental observations,<sup>15</sup> which show that TAE avalanches are present for  $\beta_{fi}(0)/\beta_{total}(0) > 0.3$  and quiescent plasmas only for  $\beta_{fi}(0)/\beta_{total}(0) < 0.3$ . As shown in Fig. 7, the mode structure, peak position, and synthetic reflectometer response are almost unaffected during the scan of fast ion central pressure.

In the conventional paradigm of the MHD theory, a TAE in a torus lies in a gap in the continuum at the  $q_{TAE} = (2m+1)/2n$  surface, and the frequency is  $\omega_{TAE} = v_A/2qR$ . In this sensitivity study, the  $q$  profile was varied within experimental uncertainties, for example, shifting  $q_{min}$  position or changing the  $q$  profile shape, to check how it affects the simulated mode peak location and mode frequency. One example is shown in Fig. 8, in which  $q_{min}$  value is slightly shifted up or down, and the  $q=7/6$  surface is also shifted in the radial direction between  $R = 133\text{--}136$  cm. It is observed that the peak of velocity streaming function  $U$  moves in the opposite direction as the  $q=7/6$  surface changes in the radial direction. Although there are some variations in the density perturbation profile, the changes in synthetic reflectometer response are within experimental uncertainties. They are not sensitive enough to tell which one agrees better with experimental data.

Experiments on the NSTX and simulations of TAEs on the DIII-D suggest that the TAE radial position tends to stay

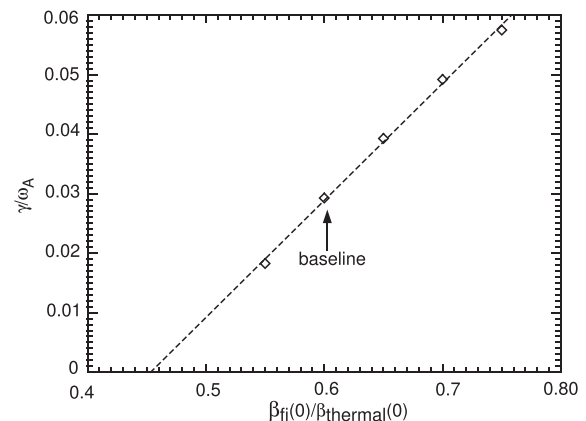


FIG. 6. The mode growth rate vs the central fast ion pressure for a set of  $n=3$  TAE simulations in which the thermal pressure is fixed, while fast ion pressure is scanned. Note that the dashed line is a linear fit and is extrapolated back to zero growth rate to find the instability threshold.

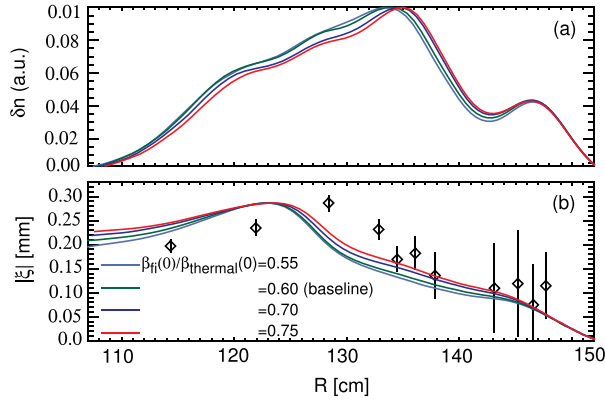


FIG. 7. Comparison of (a) density perturbation and (b) synthetic reflectometer response from a set of  $n = 3$  TAE simulations in which thermal pressure is fixed, while fast ion pressure is scanned.

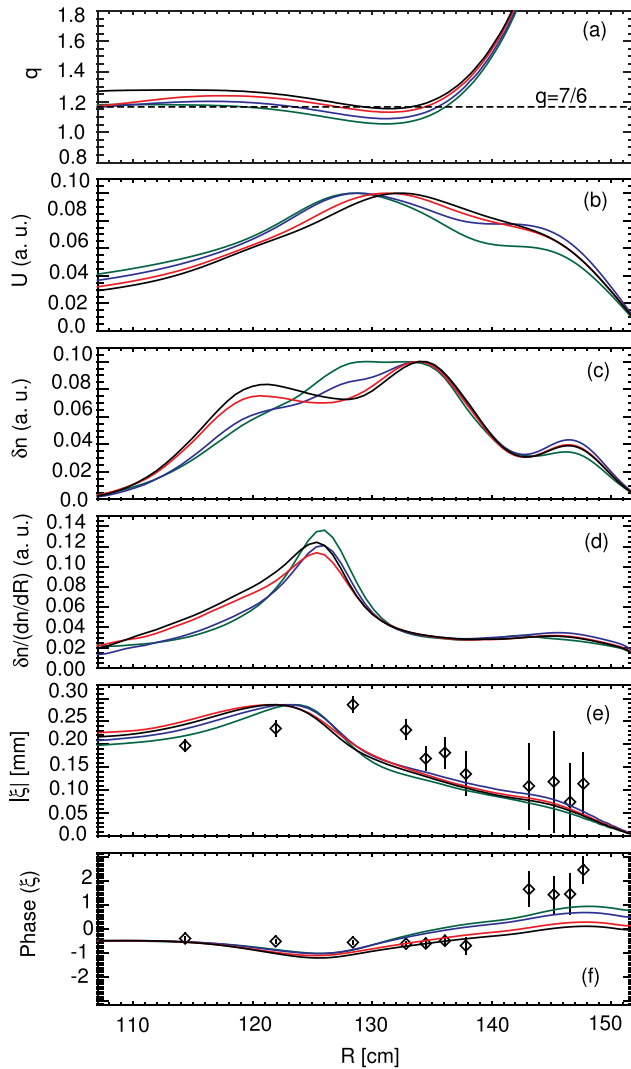


FIG. 8. Comparison of (a)  $q$  profile, (b) velocity streaming function  $U$ , (c) density perturbation, (d)  $\delta n / \nabla n$ , (e) synthetic reflectometer response, and (f) phase of a synthetic reflectometer response for a set of  $n = 3$  TAE simulations in which  $q_{\text{min}}$  position is shifted up or down and the  $q = 7/6$  surface is shifted in the radial direction correspondingly. The thermal plasma pressure profile is fixed in all runs as well as the central fast ion pressure.

around the position where the strongest fast ion pressure gradient is present.<sup>17,31</sup> In the M3D-K simulations, initial fast ion distribution is set to  $f = \frac{cH(v_0 - v)}{v^3 + v_c^3} \exp(-\langle \psi \rangle / \Delta \psi) \exp(-\frac{(\Lambda - \Lambda_0)^2}{\Delta \Lambda^2})$ . By varying the profile width  $\Delta \psi$ , we can change the fast ion pressure gradient at the  $q = 7/6$  surface. Figure 9 shows the results of M3D-K linear simulations with different fast ion profile width from  $\Delta \psi = 0.22$  to  $\Delta \psi = 0.35$ . When the fast ion pressure profile becomes broader, the fast ion pressure gradient shifts outwards. The peaks of velocity streaming function  $U$  and density perturbation also shift outward, but in a very small amount. In addition, M3D-K simulations are also performed to scan fast ion central pitch from  $\Lambda_0 = 0.40$  to  $\Lambda_0 = 0.70$  or pitch width from  $\Delta \Lambda = 0.16$  to  $\Delta \Lambda = 0.30$ . In these two scans, only very minor change is observed on the mode structure and peak position. The shift of peak position is typically less than  $< 2$  cm.

Figure 10 shows the mode growth rate versus central toroidal rotation. In this scan, the shape of toroidal rotation profile is fixed, while the peak value is re-scaled. It shows that at the experimental rotation level  $(\omega_{\text{rot}}(0) / \omega_{\text{Alfven}} = 0.245)$ , toroidal rotation starts to strongly enhance the growth rate of the mode. The exact mechanism for this enhancement is unclear. The shear rotation can affect the TAE stability in several ways. First, large toroidal rotation can significantly modify the structure of the Alfvén continuum via the Doppler shift, and thus affect the TAE mode structure and stability.<sup>32</sup> This effect is expected to be important in NSTX because of the large rotation frequency. Another possibility is the effect of rotation on wave particle resonances. Experiments from

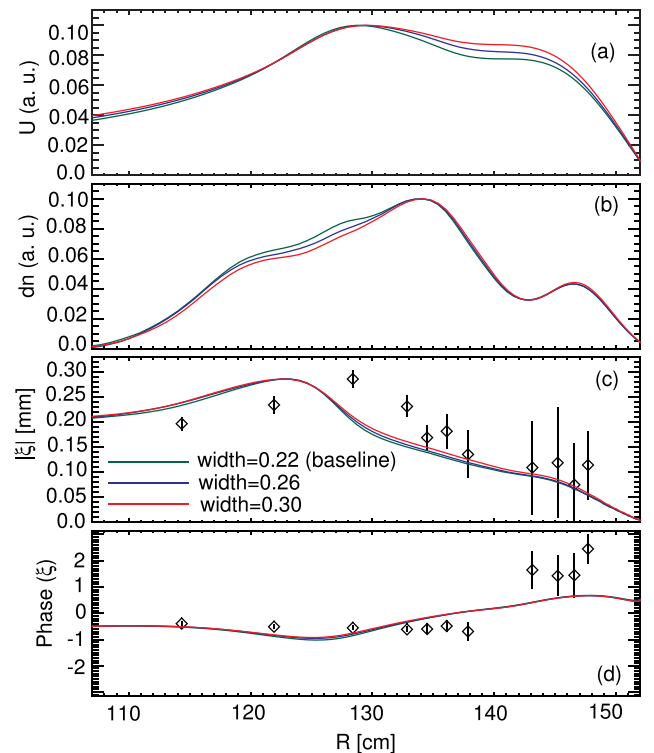


FIG. 9. Comparison of (a) velocity streaming function  $U$ , (b) density perturbation, (c) synthetic reflectometer response, and (d) phase of a synthetic reflectometer response for a set of  $n = 3$  TAE simulations in which the width of fast ion pressure profile width is scanned from  $\Delta \psi = 0.22$  to  $\Delta \psi = 0.35$ .

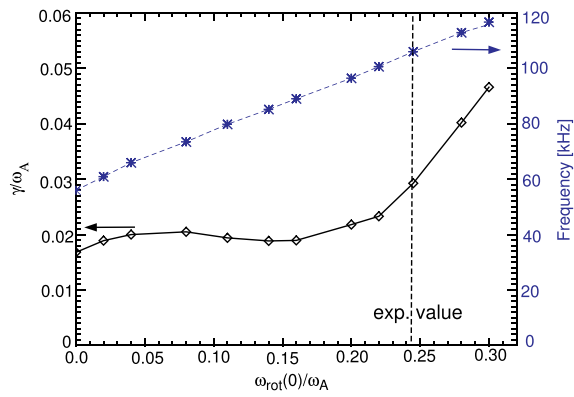


FIG. 10. The mode growth rate (solid black line with diamond symbols) and mode frequency (dashed blue line with asterisk symbols) vs the central plasma toroidal rotation for a set of  $n=3$  TAE simulations. Note that the rotational profile shape is fixed and only the magnitude is re-scaled in these runs.

conventional tokamak devices JET<sup>33</sup> and JT60-U<sup>34</sup> suggest that a strong and sheared toroidal rotation may suppress TAEs by deformation of the radial structure of the TAE mode. However, no clear experimental evidence of decorrelation of the TAE mode structure by the sheared rotation is observed on NSTX.<sup>32</sup> In addition, the shear rotation can modify energetic particle orbit and the wave particle resonances. Finally, toroidal rotation can slightly change plasma equilibrium and shift the equilibrium density profile outward, but this effect is generally small at the experimental toroidal rotation level.

As shown in Fig. 11(a), the stream function  $U$  becomes broader and shifts outward at a large toroidal rotation

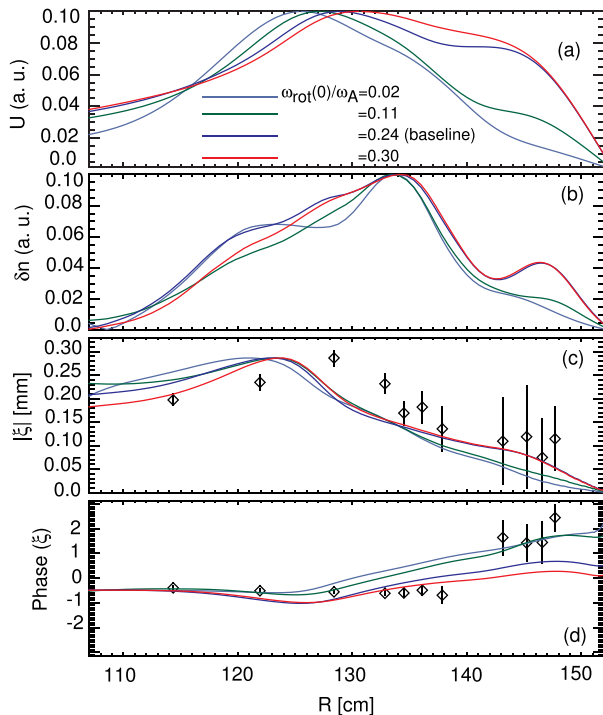


FIG. 11. Comparison of (a) velocity streaming function  $U$ , (b) density perturbation, (c) synthetic reflectometer response, and (d) phase of a synthetic reflectometer response for a set of  $n=3$  TAE simulations in which rotation amplitude is scanned.

due to the change of wave particle resonance condition and Alfvén continuum structure. The density perturbation (Fig. 11(b)) and synthetic reflectometer response (Figs. 11(c) and 11(d)) have similar trends as stream function  $U$ , but the change is relatively small. It is not very clear which one agrees significantly better with experimental measurements. Please note that the change of central toroidal rotation could significantly alter the mode frequency in lab frame via Doppler shift:  $f_{lab}^{TAE} = f_{plasma}^{TAE} + f_{Doppler}^{TAE}$ . Only when the input rotation is around the experimental level does the simulated mode frequency match the measured mode frequency.

## V. CONCLUSION AND FUTURE WORK

The kinetic/MHD hybrid code M3D-K has been successfully applied to simulate the TAE instabilities with experimental plasma parameters and profiles from the NSTX discharge #141711. Both the mode structure and mode frequency of  $n=3, 4$ , and 5 TAEs from M3D-K simulations are consistent with the experimental measurements. A systematic sensitivity study shows that the synthetic reflectometer response is relatively insensitive to variation in  $q$  profile or initial fast ion distribution (within experimental uncertainties) although the simulated streaming function  $U$  or density perturbation is somewhat more sensitive. On the other hand, the calculated mode growth depends strongly on toroidal rotation and  $q$  profile. In particular, it is found that the toroidal rotation has a significant destabilizing effect on beam-driven TAEs.

A few improvements could be made in the M3D-K simulations in the future. First, a more realistic fast ion distribution should be used as the initial fast ion distribution. In the current M3D-K simulations, the radial profile of fast ion pressure is obtained from TRANSP/NUBEAM simulations, but the energy distribution uses an analytical slowing down form. However, both the radial gradient and details of the fast ion distribution in phase space can contribute to the TAE drive. Although a full experimental measurement of the fast ion distribution in phase space is still not available, the numerical fast ion distribution from TRANSP/NUBEAM is a relatively good approximation to the realistic fast ion distribution. Experimental measurements have shown that TRANSP/NUBEAM accurately model the fast ion distribution in quiescent plasmas. Second, isolated TAE modes are simulated in this work. However, in experiments, multiple TAEs exist at the same time, which can lead to a TAE avalanche. Thus, nonlinear simulations with multiple simultaneous TAE modes and nonlinear MHD effects are desired. In addition, to capture full kinetic physics, full gyro orbit simulation is needed for fast ions.

## ACKNOWLEDGMENTS

One of the authors (D. Liu) would like to thank W. W. Hedibrink, J. Lang, W. Deng, and F. Wang for helpful discussions. This work was supported by the U.S. Department of Energy under DE-AC02-09CH11466, DE-FG02-06ER54867, and DE-FG03-02ER54681, and the simulations were performed using the supercomputer Hopper at NERSC.

- <sup>1</sup>J. Jacquinet, S. Putvinski, G. Borgia, A. Fukuyama, R. Hemsworth, S. Konovalov, Y. Nagashima, W. Nevins, K. Rasumova, F. Romanelli, K. Tobita, K. Ushigusa, J. V. Dam, V. Vdovin, and S. Zweben, *Nucl. Fusion* **39**, 2471 (1999).
- <sup>2</sup>A. Fasoli, C. Gormenzano, H. Berk, B. Breizman, S. Briguglio, D. Darrow, N. Gorelenkov, W. Heidbrink, A. Jaun, S. Konovalov, R. Nazikian, J.-M. Noterdaeme, S. Sharapov, K. Shinohara, D. Testa, K. Tobita, Y. Todo, G. Vlad, and F. Zonca, *Nucl. Fusion* **47**, S264 (2007).
- <sup>3</sup>W. Heidbrink and G. Sadler, *Nucl. Fusion* **34**, 535 (1994).
- <sup>4</sup>C. Z. Cheng and M. S. Chance, *Phys. Fluids B* **29**, 3695 (1986).
- <sup>5</sup>K. L. Wong, R. J. Fonck, S. F. Paul, D. R. Roberts, E. D. Fredrickson, R. Nazikian, H. K. Park, M. Bell, N. L. Bretz, R. Budny, S. Cohen, G. W. Hammett, F. C. Jobes, D. M. Meade, S. S. Medley, D. Mueller, Y. Nagayama, D. K. Owens, and E. J. Synakowski, *Phys. Rev. Lett.* **66**, 1874 (1991).
- <sup>6</sup>W. Heidbrink, E. Strait, E. Doyle, G. Sager, and R. Snider, *Nucl. Fusion* **31**, 1635 (1991).
- <sup>7</sup>W. W. Heidbrink, *Phys. Plasmas* **15**, 055501 (2008).
- <sup>8</sup>D. A. Spong, E. M. Bass, W. Deng, W. W. Heidbrink, Z. Lin, B. Tobias, M. A. Van Zeeland, M. E. Austin, C. W. Domier, and N. C. Luhmann, *Phys. Plasmas* **19**, 082511 (2012).
- <sup>9</sup>W. Deng, Z. Lin, I. Holod, Z. Wang, Y. Xiao, and H. Zhang, *Nucl. Fusion* **52**, 043006 (2012).
- <sup>10</sup>Y. Chen, T. Munsat, S. E. Parker, W. W. Heidbrink, M. A. Van Zeeland, B. J. Tobias, and C. W. Domier, *Phys. Plasmas* **20**, 012109 (2013).
- <sup>11</sup>E. M. Bass and R. E. Waltz, *Phys. Plasmas* **20**, 012508 (2013).
- <sup>12</sup>G. Y. Fu, W. Park, H. R. Strauss, J. Breslau, J. Chen, S. Jardin, and L. E. Sugiyama, *Phys. Plasmas* **13**, 052517 (2006).
- <sup>13</sup>M. Ono, S. Kaye, Y.-K. Peng, G. Barnes, W. Blanchard, M. Carter, J. Chrzanowski, L. Dudek, R. Ewig, D. Gates, R. Hatcher, T. Jarboe, S. Jardin, D. Johnson, R. Kaita, M. Kalish, C. Kessel, H. Kugel, R. Maingi, R. Majeski, J. Manickam, B. McCormack, J. Menard, D. Mueller, B. Nelson, B. Nelson, C. Neumeyer, G. Oliaro, F. Paoletti, R. Parsells, E. Perry, N. Pomphrey, S. Ramakrishnan, R. Raman, G. Rewoldt, J. Robinson, A. Roquemore, P. Ryan, S. Sabbagh, D. Swain, E. Synakowski, M. Viola, M. Williams, J. Wilson, and NSTX Team, *Nucl. Fusion* **40**, 557 (2000).
- <sup>14</sup>E. Fredrickson, N. Gorelenkov, R. Bell, J. Menard, A. Roquemore, S. Kubota, N. Crocker, and W. Peebles, *Nucl. Fusion* **46**, S926 (2006).
- <sup>15</sup>E. Fredrickson, N. Gorelenkov, M. Podesta, A. Bortolon, S. Gerhardt, R. Bell, A. Diallo, and B. LeBlanc, *Nucl. Fusion* **54**, 093007 (2014).
- <sup>16</sup>E. D. Fredrickson, N. A. Crocker, R. E. Bell, D. S. Darrow, N. N. Gorelenkov, G. J. Kramer, S. Kubota, F. M. Levinton, D. Liu, S. S. Medley, M. Podesta, K. Tritz, R. B. White, and H. Yuh, *Phys. Plasmas* **16**, 122505 (2009).
- <sup>17</sup>M. Podesta, R. Bell, A. Bortolon, N. Crocker, D. Darrow, A. Diallo, E. Fredrickson, G.-Y. Fu, N. Gorelenkov, W. Heidbrink, G. Kramer, S. Kubota, B. LeBlanc, S. Medley, and H. Yuh, *Nucl. Fusion* **52**, 094001 (2012).
- <sup>18</sup>E. Fredrickson, N. Crocker, D. Darrow, N. Gorelenkov, G. Kramer, S. Kubota, M. Podesta, R. White, A. Bortolon, S. Gerhardt, R. Bell, A. Diallo, B. LeBlanc, F. Levinton, and H. Yuh, *Nucl. Fusion* **53**, 013006 (2013).
- <sup>19</sup>J. Lang, G.-Y. Fu, and Y. Chen, *Phys. Plasmas* **17**, 042309 (2010).
- <sup>20</sup>H. Cai and G. Fu, *Phys. Plasmas* **19**, 072506 (2012).
- <sup>21</sup>F. Wang, G. Y. Fu, J. A. Breslau, K. Tritz, and J. Y. Liu, *Phys. Plasmas* **20**, 072506 (2013).
- <sup>22</sup>F. Wang, G. Y. Fu, J. A. Breslau, and J. Y. Liu, *Phys. Plasmas* **20**, 102506 (2013).
- <sup>23</sup>J. Lang, G.-Y. Fu, Y. Chen, J. Breslau, J. Chen, G. Kramer, and M. Van Zeeland, in APS Meeting Abstracts (2011).
- <sup>24</sup>A. Pankin, D. McCune, R. Andre, G. Bateman, and A. Kritz, *Comput. Phys. Commun.* **159**, 157 (2004).
- <sup>25</sup>R. Hawryluk, *Physics of Plasmas Close to Thermonuclear Conditions*, edited by B. Coppi, G. G. Leotta, D. Pfirsch, R. Pozzoli, and E. Sindoni (CEC, Brussels, 1980), Vol. 1.
- <sup>26</sup>J. E. Menard, R. E. Bell, D. A. Gates, S. M. Kaye, B. P. LeBlanc, F. M. Levinton, S. S. Medley, S. A. Sabbagh, D. Stutman, K. Tritz, and H. Yuh, *Phys. Rev. Lett.* **97**, 095002 (2006).
- <sup>27</sup>F. M. Levinton and H. Yuh, *Rev. Sci. Instrum.* **79**, 10F522 (2008).
- <sup>28</sup>N. A. Crocker, W. A. Peebles, S. Kubota, J. Zhang, R. E. Bell, E. D. Fredrickson, N. N. Gorelenkov, B. P. LeBlanc, J. E. Menard, M. Podesta, S. A. Sabbagh, K. Tritz, and H. Yuh, *Plasma Phys. Controlled Fusion* **53**, 105001 (2011).
- <sup>29</sup>W. W. Heidbrink, *Rev. Sci. Instrum.* **81**, 10D727 (2010).
- <sup>30</sup>R. E. Bell, R. Andre, S. M. Kaye, R. A. Kolesnikov, B. P. LeBlanc, G. Rewoldt, W. X. Wang, and S. A. Sabbagh, *Phys. Plasmas* **17**, 082507 (2010).
- <sup>31</sup>Z. Wang, Z. Lin, I. Holod, W. W. Heidbrink, B. Tobias, M. Van Zeeland, and M. E. Austin, *Phys. Rev. Lett.* **111**, 145003 (2013).
- <sup>32</sup>M. Podesta, R. E. Bell, E. D. Fredrickson, N. N. Gorelenkov, B. P. LeBlanc, W. W. Heidbrink, N. A. Crocker, S. Kubota, and H. Yuh, *Phys. Plasmas* **17**, 122501 (2010).
- <sup>33</sup>D. Testa, C. Boswell, A. Fasoli, and JET-EFDA Contributors, *Nucl. Fusion* **45**, 907 (2005).
- <sup>34</sup>M. Saigusa, Y. Kusama, T. Ozeki, H. Kimura, T. Fujita, S. Moriyama, T. Fujii, M. Azumi, V. Afanassiev, Y. Neyatani, G. Fu, and C. Cheng, *Nucl. Fusion* **37**, 1559 (1997).